


 Cite this: *RSC Adv.*, 2025, **15**, 28651

## Rare earth doping: a strategy to enhance the catalytic activity of $\text{ZnFe}_2\text{O}_4$ in activating peroxyomonosulfate for acetaminophen degradation

 Hangdao Qin, <sup>a</sup> Lei Xiao, <sup>a</sup> Junnan Hao, <sup>a</sup> Yong Wang, <sup>a</sup> Jiming Huang, <sup>a</sup> Guo Yang<sup>b</sup> and Bo Xing<sup>b</sup>

In this paper,  $\text{ZnFe}_2\text{O}_4$  was doped by two rare earth metals (La and Pr), and the as-prepared  $\text{ZnLa}_{0.5}\text{Fe}_{1.5}\text{O}_4$  and  $\text{ZnPr}_{0.5}\text{Fe}_{1.5}\text{O}_4$  were applied to activate PMS for acetaminophen degradation.  $\text{ZnLa}_{0.5}\text{Fe}_{1.5}\text{O}_4$  with the largest oxygen vacancy ( $\text{O}_v$ ) content showed the highest acetaminophen degradation efficacy. About 89.7% of acetaminophen was removed within 60 min in the  $\text{ZnLa}_{0.5}\text{Fe}_{1.5}\text{O}_4/\text{PMS}$  system. Free radical quenching experiments and EPR tests confirmed that  $\text{SO}_4^{\cdot-}$ ,  $\cdot\text{OH}$ ,  $\text{O}_2^{\cdot-}$  and  ${}^1\text{O}_2$  were the dominant reactive oxygen species (ROS). The role of La/Pr doping was explored through a series of comparative studies. The results indicated that La doping enhanced the content of oxygen vacancies, accelerated the electron transfer in the system, and thus sharply improved the catalytic performance of  $\text{ZnFe}_2\text{O}_4$ . Furthermore, the reusability, universality and actual water environment adaptability of  $\text{ZnLa}_{0.5}\text{Fe}_{1.5}\text{O}_4$  were investigated.

Received 14th July 2025

Accepted 4th August 2025

DOI: 10.1039/d5ra05044h

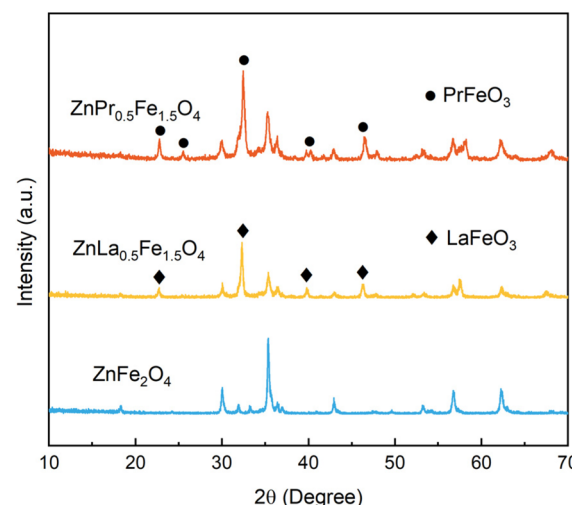
[rsc.li/rsc-advances](http://rsc.li/rsc-advances)

### 1. Introduction

Sulfate radical-based advanced oxidation processes (SR-AOPs) have been proved to effectively eliminate pharmaceuticals and personal care products (PPCPs) in water due to the generation of powerful reactive oxygen species (ROS) in the presence of catalysts.<sup>1</sup>  $\text{ZnFe}_2\text{O}_4$  is a bimetallic oxide with spinel structure ( $\text{AB}_2\text{O}_4$ ), and bivalent  $\text{Zn}^{2+}$  occupies the A-site and trivalent  $\text{Fe}^{3+}$  occupies the B-site. Magnetic nanostructured  $\text{ZnFe}_2\text{O}_4$  is a highly efficient and environmentally friendly catalyst in activating peroxyomonosulfate (PMS) for the degradation of organic pollutants.<sup>2,3</sup>

To further improve the catalytic performance of  $\text{ZnFe}_2\text{O}_4$ , metal cation doping has been proved to be a feasible method.<sup>4-6</sup> Mn-doped  $\text{ZnFe}_2\text{O}_4$  ( $\text{Mn}_{0.6}\text{Zn}_{0.4}\text{Fe}_2\text{O}_4$ ) was prepared using spent Zn-Mn alkaline batteries, and its catalytic performance was higher than that of  $\text{ZnFe}_2\text{O}_4$  and  $\text{MnFe}_2\text{O}_4$  in activating PMS for bisphenol A degradation.<sup>4</sup> In the previous work of the authors, Ni-doped  $\text{ZnFe}_2\text{O}_4$  ( $\text{Ni}_{0.5}\text{Zn}_{0.5}\text{Fe}_2\text{O}_4$ ) was synthesized and applied to activate PMS for the decay of cefotaxime sodium.<sup>5</sup> The results indicated that the synergistic effect between  $\text{Ni}^{2+}$  and  $\text{Zn}^{2+}$  accelerated the  $\text{Fe}^{3+}/\text{Fe}^{2+}$  cycle, and thus promoted the generation of ROS in the system. In another report, Cu

substituted  $\text{ZnFe}_2\text{O}_4$  was successfully prepared and used for PMS activation to degrade ciprofloxacin.<sup>6</sup> The excellent catalytic activity was due to the generated large amount of oxygen vacancies after Cu substitution. Oxygen vacancies were also the main active sites for PMS activation to produce ROS. It could be concluded that doping could not only accelerate the electron transfer in the system by the synergistic effect between metals, but also regulate the generation of oxygen vacancies in  $\text{ZnFe}_2\text{O}_4$ ,


 Fig. 1 XRD patterns of  $\text{ZnFe}_2\text{O}_4$ ,  $\text{ZnLa}_{0.5}\text{Fe}_{1.5}\text{O}_4$  and  $\text{ZnPr}_{0.5}\text{Fe}_{1.5}\text{O}_4$ .

<sup>a</sup>School of Material and Chemical Engineering, Tongren University, Tongren 554300, China. E-mail: qinhangdao@126.com

<sup>b</sup>College of Chemical Engineering, Sichuan University of Science and Engineering, Zigong 643000, China



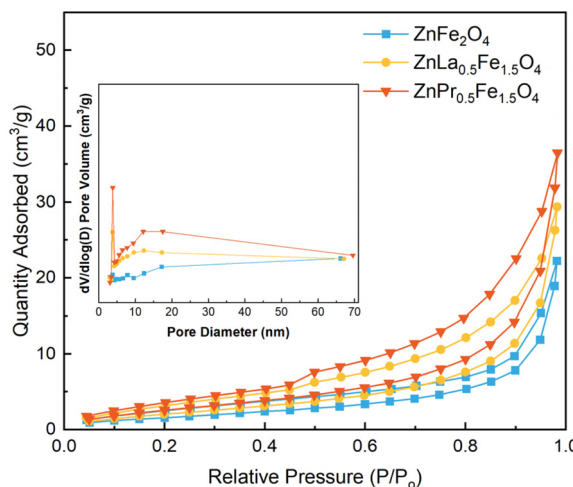


Fig. 2 N<sub>2</sub> adsorption–desorption isotherms and pore size distribution curves of ZnFe<sub>2</sub>O<sub>4</sub>, ZnLa<sub>0.5</sub>Fe<sub>1.5</sub>O<sub>4</sub> and ZnPr<sub>0.5</sub>Fe<sub>1.5</sub>O<sub>4</sub>.

Table 1 The BET surface area, pore volume and average pore size of catalysts

Catalysts	BET surface area (m <sup>2</sup> g <sup>-1</sup> )	Pore volume (cm <sup>3</sup> g <sup>-1</sup> )	Average pore size (nm)
ZnFe <sub>2</sub> O <sub>4</sub>	8	0.033	3.07
ZnLa <sub>0.5</sub> Fe <sub>1.5</sub> O <sub>4</sub>	15	0.046	3.82
ZnPr <sub>0.5</sub> Fe <sub>1.5</sub> O <sub>4</sub>	20	0.058	3.82

which was beneficial to promote the production of ROS in the catalytic system. Oxygen vacancies were curial.

However, all the above reports were focused on A-site doping, the effect of B-site doping on the catalytic performance of ZnFe<sub>2</sub>O<sub>4</sub> was rarely investigated. In this study, trivalent rare earth ions (La<sup>3+</sup> and Pr<sup>3+</sup>) were used to partly substitute Fe<sup>3+</sup> in

B-site. The as-prepared catalysts were applied to activate PMS for the degradation of acetaminophen which was a widely used antipyretic and analgesic pharmaceutical.<sup>7</sup> The effect of rare earth cation doping on the microstructure, oxygen vacancies and catalytic activity was studied based on the catalyst characterization and activity evaluation. Furthermore, the produced ROS were determinated and the role of La/Pr doping was investigated based on a series of comparative studies including X-ray photoelectron spectra (XPS) analysis, electron paramagnetic resonance (EPR) tests and electrochemical analysis. Finally, the reusability, universality and actual water environment adaptability of the catalyst were investigated to evaluate the potential of practical applications of the catalyst.

## 2. Experimental

### 2.1. Catalyst preparation and characterization

The sourcing and purity information of the used chemicals in this study are mentioned in Text S1 in the SI.

La/Pr-doped ZnFe<sub>2</sub>O<sub>4</sub> was prepared by sol-gel self-combustion method. The detailed synthesis process was described in the previous study.<sup>8</sup> Synthesis schematic depiction of ZnLa<sub>0.5</sub>Fe<sub>1.5</sub>O<sub>4</sub>/ZnPr<sub>0.5</sub>Fe<sub>1.5</sub>O<sub>4</sub> catalyst has been added in Fig. S1 in the SI. Took ZnLa<sub>0.5</sub>Fe<sub>1.5</sub>O<sub>4</sub> as an example. Analytical grade Zn(NO<sub>3</sub>)<sub>2</sub>·9H<sub>2</sub>O, Fe(NO<sub>3</sub>)<sub>3</sub>·9H<sub>2</sub>O and La(NO<sub>3</sub>)<sub>3</sub>·6H<sub>2</sub>O were accurately weighed in stoichiometric proportions, and then dissolved in distilled water. Citric acid was added into each sample of metal nitrates in 1:1 molar ratio of citric acid to metal ions. The above solutions were heated for 5 h at 70 °C through gel phase transformation. The dry gel was obtained after aging and drying, and then ground into powder and heat-treated at 500 °C for 2 h in a muffle furnace with the heating rate of 10 °C min<sup>-1</sup>. La(NO<sub>3</sub>)<sub>3</sub>·6H<sub>2</sub>O was replaced with Pr(NO<sub>3</sub>)<sub>3</sub>·5H<sub>2</sub>O when preparing ZnPr<sub>0.5</sub>Fe<sub>1.5</sub>O<sub>4</sub>. Undoped ZnFe<sub>2</sub>O<sub>4</sub>, as a control, was synthesized using the same procedure without adding dopant. The detailed information including

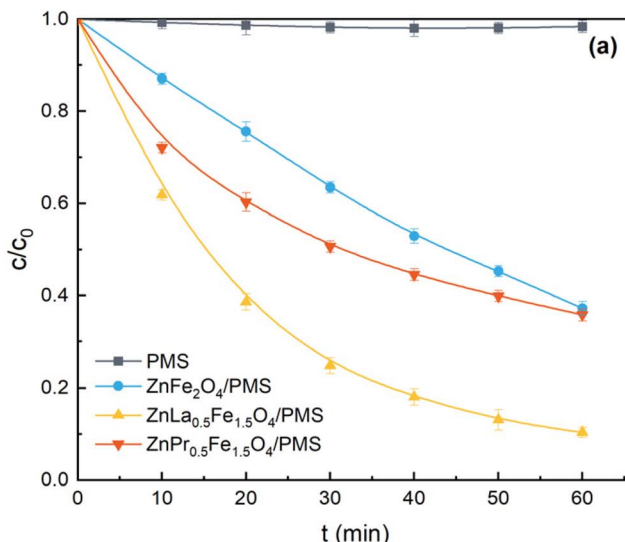
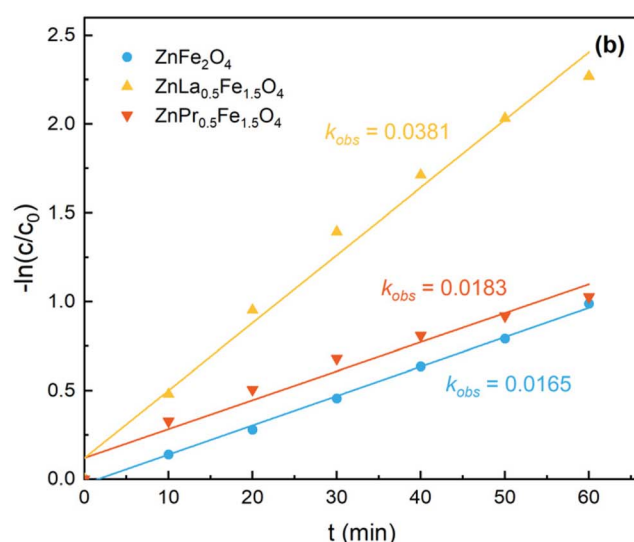


Fig. 3 (a) Acetaminophen degradation in different systems; (b) acetaminophen degradation kinetics. Reaction conditions: [acetaminophen]<sub>0</sub> = 20 mg L<sup>-1</sup>, [PMS]<sub>0</sub> = 1.0 g L<sup>-1</sup>, [catalyst]<sub>0</sub> = 1.0 g L<sup>-1</sup>, unadjusted pH = 6.98, T = 25 °C.



**Table 2** The  $\text{ZnLa}_{0.5}\text{Fe}_{1.5}\text{O}_4$  catalyst compared with other catalysts used in acetaminophen degradation

Catalyst	Oxidizing reagent	Removal	References
$\text{ZnLa}_{0.5}\text{Fe}_{1.5}\text{O}_4$	PMS	89.7%	This study
Co/EMR	$\text{H}_2\text{O}_2$	63.8%	Qin <i>et al.</i> <sup>7</sup>
Fe-g-C <sub>3</sub> N <sub>4</sub>	$\text{H}_2\text{O}_2$	98.1%	Mu <i>et al.</i> <sup>11</sup>
C/TiO <sub>2</sub>	PDS	100%	Dang <i>et al.</i> <sup>12</sup>
FeMo@NCN	PMS	72.0%	Huang <i>et al.</i> <sup>13</sup>
FeCe <sub>0.05</sub> /BC	PMS	99.9%	Du <i>et al.</i> <sup>14</sup>

instruments and methods used in catalyst characterization was shown in Text S2 in the SI.

## 2.2. Degradation experiments and analytical methods

The degradation experiments were carried out in a 250 mL conical flask, which was placed in a constant temperature air bath shaker. The temperature and the rotate speed were set at 25 °C and 300 rpm, respectively. In each experiment, 100 mg of solid catalyst was introduced into 100 mL of 20 mg L<sup>-1</sup> acetaminophen solution. Then 100 mg of PMS was introduced into the system to initial the oxidation reaction. Samples were extracted at specific time intervals and immediately filtered through a 0.45 µm membrane for further analysis. The detailed experimental procedure for the recycle study was shown in Text S3 in the SI. The analytical methods were described in detail in Text S4 in the SI. The details of operational approach of electrochemical impedance spectroscopy (EIS) and open-circuit potential (OCP) were presented in Text S5 in the SI.

## 3. Results and discussion

### 3.1. Characterization

The X-ray diffraction (XRD) patterns of the as-prepared catalysts are shown in Fig. 1. All of these catalysts exhibited a pure cubic

crystal structure of franklinite (JCPDS No. 89-4926). Some new peaks appeared after doping, which corresponded to the crystal planes of  $\text{LaFeO}_3$  (JCPDS No. 88-0641) and  $\text{PrFeO}_3$  (JCPDS No. 47-0065) with perovskite structure.<sup>9,10</sup> These results indicated that a composite of spinel  $\text{ZnFe}_2\text{O}_4$  and perovskite  $\text{LaFeO}_3/\text{PrFeO}_3$  was formed when parts of framework Fe were substituted by La/Pr.

The  $\text{N}_2$  adsorption–desorption isotherms and pore size distribution curves of catalysts are presented in Fig. 2. All the isotherms possessed the type IV curve with an H3 type hysteresis loop, which suggested a mesoporous structure of the four catalysts. Moreover, the pore size distribution curves indicated that the pore size basically concentrated in the range of 1–20 nm. The BET surface area was calculated from the Brunauer–Emmett–Teller (BET) method, and the total pore volume was determined by the near saturation uptake ( $P/P_0 = 0.99$ ). The average pore size was calculated using Barrett–Joyner–Halenda (BJH) method. As seen from Table 1 that rare earth doping enhanced the surface area and pore volume, and  $\text{ZnPr}_{0.5}\text{Fe}_{1.5}\text{O}_4$  showed higher BET surface area (20 m<sup>2</sup> g<sup>-1</sup>) and pore volume (0.058 cm<sup>3</sup> g<sup>-1</sup>).

### 3.2. Removal of acetaminophen in different systems

The adsorption of acetaminophen by different catalysts was investigated (Fig. S2), and the results indicated that adsorption could hardly remove acetaminophen. As shown in Fig. 3a, single PMS had low degradation ability for acetaminophen, since only 1.2% of acetaminophen was removed within 60 min. The degradation rate of acetaminophen was 62.8% in  $\text{ZnFe}_2\text{O}_4/\text{PMS}$  system. La/Pr doping improved the catalytic performance, and  $\text{ZnLa}_{0.5}\text{Fe}_{1.5}\text{O}_4/\text{PMS}$  system (89.7%) showed higher acetaminophen degradation efficiency than that of  $\text{ZnPr}_{0.5}\text{Fe}_{1.5}\text{O}_4/\text{PMS}$  system (64.2%). Moreover, according to Fig. 3b, the degradation of acetaminophen could be well fitted by the pseudo-first-order kinetic. The  $k_{\text{obs}}$  was calculated to be 0.0165, 0.0183 and 0.0381 min<sup>-1</sup> for  $\text{ZnFe}_2\text{O}_4$ ,  $\text{ZnLa}_{0.5}\text{Fe}_{1.5}\text{O}_4$  and  $\text{ZnPr}_{0.5}\text{Fe}_{1.5}\text{O}_4$ ,

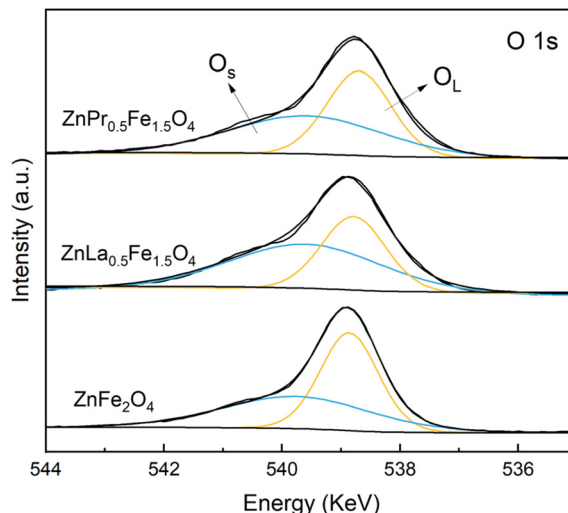


**Fig. 4** O 1s XPS spectra of  $\text{ZnFe}_2\text{O}_4$ ,  $\text{ZnLa}_{0.5}\text{Fe}_{1.5}\text{O}_4$  and  $\text{ZnPr}_{0.5}\text{Fe}_{1.5}\text{O}_4$ .

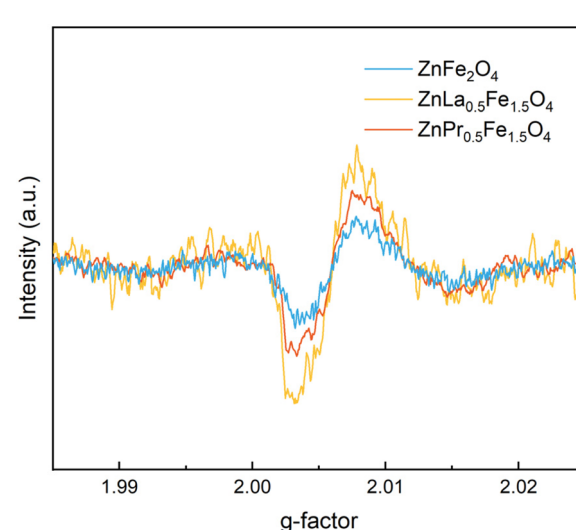


**Fig. 5** EPR spectra of  $\text{ZnFe}_2\text{O}_4$ ,  $\text{ZnLa}_{0.5}\text{Fe}_{1.5}\text{O}_4$  and  $\text{ZnPr}_{0.5}\text{Fe}_{1.5}\text{O}_4$ .



respectively. The catalytic performances followed the order of  $\text{ZnFe}_2\text{O}_4 < \text{ZnPr}_{0.5}\text{Fe}_{1.5}\text{O}_4 < \text{ZnLa}_{0.5}\text{Fe}_{1.5}\text{O}_4$ .

Besides, the  $\text{ZnLa}_{0.5}\text{Fe}_{1.5}\text{O}_4$  catalyst obtained in the present study was compared with other catalysts used in acetaminophen degradation (Table 2). Although all the catalysts were used in AOPs for the degradation of acetaminophen, the oxidizing reagents and reaction conditions were different, and thus a true quantity comparison was impossible.

### 3.3. The role of La/Pr doping

**3.3.1 Influence of oxygen vacancies.** It was observed that there was a lack of linear correlation between catalytic performance and BET surface area (Table 1). Therefore, in order to explore the role of La/Pr doping, a series of comparative studies including XPS analysis, EPR tests and electrochemical analysis were conducted.

Firstly, XPS analysis and EPR tests were conducted to clarify the relationship between the doping elements and oxygen vacancies in the catalysts. The XPS survey spectra of  $\text{ZnFe}_2\text{O}_4$ ,  $\text{ZnLa}_{0.5}\text{Fe}_{1.5}\text{O}_4$  and  $\text{ZnPr}_{0.5}\text{Fe}_{1.5}\text{O}_4$  were presented in Fig. S3 in the SI.  $\text{ZnLa}_{0.5}\text{Fe}_{1.5}\text{O}_4$  consisted of Zn, Fe, La and O elements and  $\text{ZnPr}_{0.5}\text{Fe}_{1.5}\text{O}_4$  consisted of Zn, Fe, Pr and O elements, which further confirmed that La/Pr was successfully doped onto  $\text{ZnFe}_2\text{O}_4$ . The fine-scanned XPS spectra of O 1 s were shown in Fig. 4. The peaks at 538.6 eV and 539.5 eV were assigned to lattice oxygen ( $\text{O}_L$ ) and adsorbed oxygen or surface oxygen ( $\text{O}_S$ ), respectively. The ratio of  $\text{O}_S/\text{O}_L$  was closely related to oxygen vacancies, and the high ratio signified more oxygen vacancies over the catalyst surface.<sup>15</sup> The calculated ratios were 0.85, 1.54 and 1.14 for  $\text{ZnFe}_2\text{O}_4$ ,  $\text{ZnLa}_{0.5}\text{Fe}_{1.5}\text{O}_4$  and  $\text{ZnPr}_{0.5}\text{Fe}_{1.5}\text{O}_4$ , respectively.  $\text{ZnLa}_{0.5}\text{Fe}_{1.5}\text{O}_4$  possessed the most oxygen vacancies, while the content of oxygen vacancies in  $\text{ZnFe}_2\text{O}_4$  was smallest.

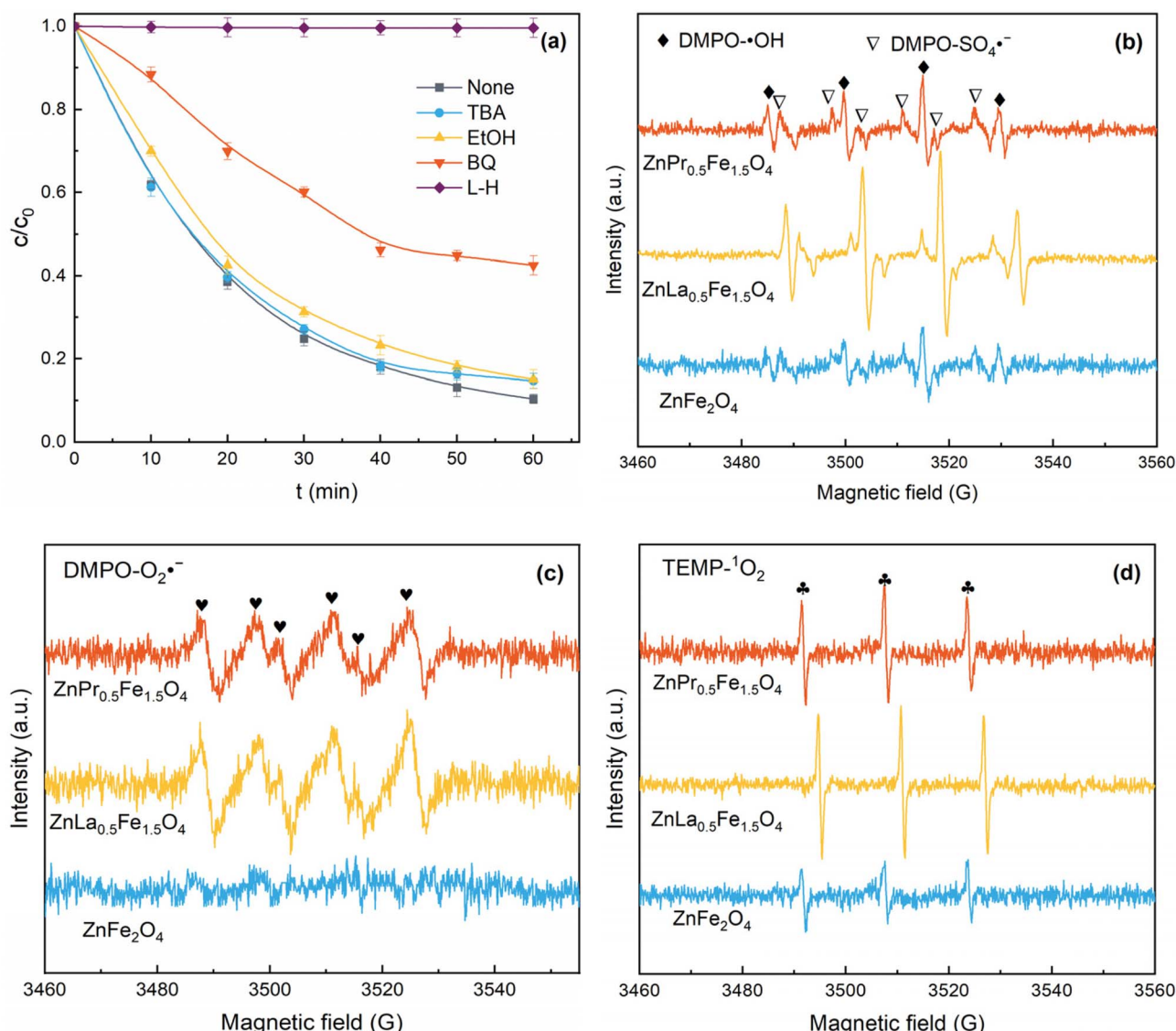


Fig. 6 (a) Quenching experiments; EPR spectra of  $\cdot\text{OH}$  and  $\text{SO}_4^{\cdot-}$  (b),  $\text{O}_2^{\cdot-}$  (c), and  ${}^1\text{O}_2$  (d). Reaction conditions:  $[\text{acetaminophen}]_0 = 20 \text{ mg L}^{-1}$ ,  $[\text{PMS}]_0 = 1.0 \text{ g L}^{-1}$ ,  $[\text{catalyst}]_0 = 1.0 \text{ g L}^{-1}$ ,  $[\text{TBA}] = [\text{EtOH}] = [\text{BQ}] = [\text{L-H}] = 10 \text{ mM}$ , unadjusted pH = 6.98,  $T = 25^\circ\text{C}$ .



Moreover, as presented in Fig. 5, the intensity of the EPR signals followed the order of  $\text{ZnFe}_2\text{O}_4 < \text{ZnPr}_{0.5}\text{Fe}_{1.5}\text{O}_4 < \text{ZnLa}_{0.5}\text{Fe}_{1.5}\text{O}_4$ . Based on the results of XPS analysis and EPR tests, it could be concluded that as same as A-site doping, B-site doping with rare earth also could tune the oxygen vacancies in  $\text{ZnFe}_2\text{O}_4$  catalyst, and the oxygen vacancies were increased by the incorporation of rare earth into the lattice. It was important that the catalytic activity was increased with the concentration of oxygen vacancies in the catalysts, which indicated oxygen vacancies were the active sites for the activation of PMS.<sup>16</sup>

**3.3.2 ROS determination.** It was known that PMS could be activated to produce ROS to oxidize organic pollutants. Free radicals quenching experiments were performed to determinate the generated ROS in  $\text{ZnLa}_{0.5}\text{Fe}_{1.5}\text{O}_4/\text{PMS}$  system, and the results were illustrated in Fig. 6a. The degradation of acetaminophen was almost completely inhibited when L-Histidine (L-H) was introduced. The addition of benzoquinone (BQ) apparently prevented the removal of acetaminophen. However, after adding *tert*-butanol (TBA) or ethanol (EtOH) into the system, the acetaminophen degradation rate declined slightly. These results suggested  $\text{O}_2^{\cdot-}$  and  $^1\text{O}_2$  contributed more than  $\text{SO}_4^{\cdot-}$  and  $\cdot\text{OH}$  for the decay of acetaminophen.

Moreover, EPR measurements were used to further confirm the ROS generated during the catalytic process. In Fig. 6b, 5,5-dimethyl-1-pyrroline-N-oxide (DMPO) was used as a radical trapping agent for  $\text{SO}_4^{\cdot-}$  and  $\cdot\text{OH}$ , and DMPO- $\text{SO}_4^{\cdot-}$  and DMPO- $\cdot\text{OH}$  signals were observed, which indicated both  $\text{SO}_4^{\cdot-}$  and  $\cdot\text{OH}$  were generated in  $\text{ZnLa}_{0.5}\text{Fe}_{1.5}\text{O}_4/\text{PMS}$  system. As shown in Fig. 6c, DMPO was used as a radical trapping agent for  $\text{O}_2^{\cdot-}$ , and the characteristic signal for DMPO- $\text{O}_2^{\cdot-}$  adducts confirmed the generation of  $\text{O}_2^{\cdot-}$  in  $\text{ZnLa}_{0.5}\text{Fe}_{1.5}\text{O}_4/\text{PMS}$  system. As exhibited in Fig. 6d, 2,2,6,6-tetramethyl-4-piperidone (TEMP) was employed as a radical trapping agent for  $^1\text{O}_2$ , and the typical 1:1:1 triplet signals of TEMP- $^1\text{O}_2$  were detected, which further demonstrated the existence of  $^1\text{O}_2$  in  $\text{ZnLa}_{0.5}\text{Fe}_{1.5}\text{O}_4/\text{PMS}$  system. Besides, the signal intensity of  $\text{ZnLa}_{0.5}\text{Fe}_{1.5}\text{O}_4$  was

higher than that of  $\text{ZnFe}_2\text{O}_4$  and  $\text{ZnPr}_{0.5}\text{Fe}_{1.5}\text{O}_4$ , which was the reason for the highest catalytic performance of  $\text{ZnLa}_{0.5}\text{Fe}_{1.5}\text{O}_4$ . La/Pr doping enhanced the content of oxygen vacancies, and thus accelerated the production of ROS, which was ascribed to the fact that oxygen vacancies could facilitate the adsorption of PMS on catalyst surface.<sup>17</sup>

### 3.3.3 Confirmation of direct electron transfer pathway.

Except for oxidizing by ROS, the electron transfer pathway might be involved in the degradation of organic contaminations. On the other hand, the oxygen vacancies could facilitate the interfacial electron transfer of the catalyst,<sup>18</sup> so the electrochemical impedance spectroscopy (EIS) was used to determinate the charge transfer resistances for the three catalysts. As shown in Fig. 7a, the charge transfer resistance ( $R_{ct}$ ) obtained from equivalent circuit fitting was 7368, 824.1 and 2325  $\Omega$  for  $\text{ZnFe}_2\text{O}_4$ ,  $\text{ZnLa}_{0.5}\text{Fe}_{1.5}\text{O}_4$  and  $\text{ZnPr}_{0.5}\text{Fe}_{1.5}\text{O}_4$ , respectively. The results demonstrated that La/Pr doping elevated electronic conductivity and charge transfer efficiency. Therefore, La/Pr doping was able to enhance the reaction kinetic performance of the catalytic system by lowing the charge transfer barrier. In addition, the electron transformation ability followed the order of  $\text{ZnLa}_{0.5}\text{Fe}_{1.5}\text{O}_4 > \text{ZnPr}_{0.5}\text{Fe}_{1.5}\text{O}_4 > \text{ZnFe}_2\text{O}_4$ , which was the same as the order of the content of oxygen vacancies in the three catalysts.

Moreover, the charge transfer among PMS, catalyst and acetaminophen was also explored through the open-circuit potential (OCP) curves. As illustrated in Fig. 7b, after the addition of acetaminophen into the different catalytic systems, an obvious decline of potential was observed, which was ascribed to the donation of electrons by acetaminophen. The potential dropped due to the decomposition of PMS and the oxidation of metal ions.<sup>16</sup> The potential difference was 0.0367 V, 0.0654 V and 0.0619 V in  $\text{ZnFe}_2\text{O}_4/\text{PMS}$  system,  $\text{ZnLa}_{0.5}\text{Fe}_{1.5}\text{O}_4/\text{PMS}$  system and  $\text{ZnPr}_{0.5}\text{Fe}_{1.5}\text{O}_4/\text{PMS}$  system, respectively. The potential difference in the  $\text{ZnLa}_{0.5}\text{Fe}_{1.5}\text{O}_4/\text{PMS}$  system was the

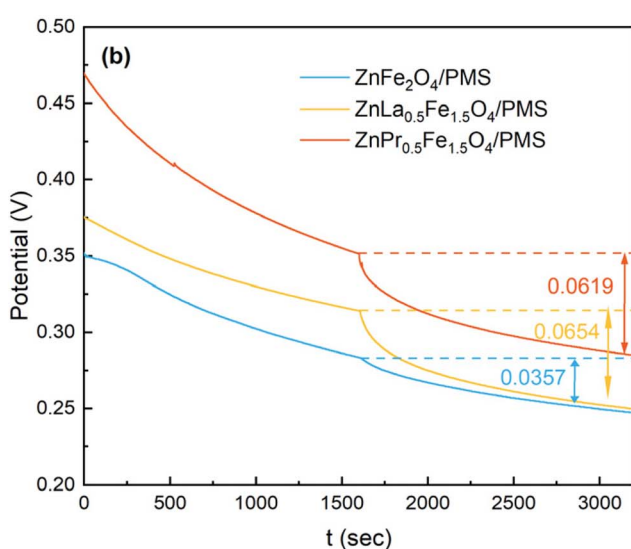
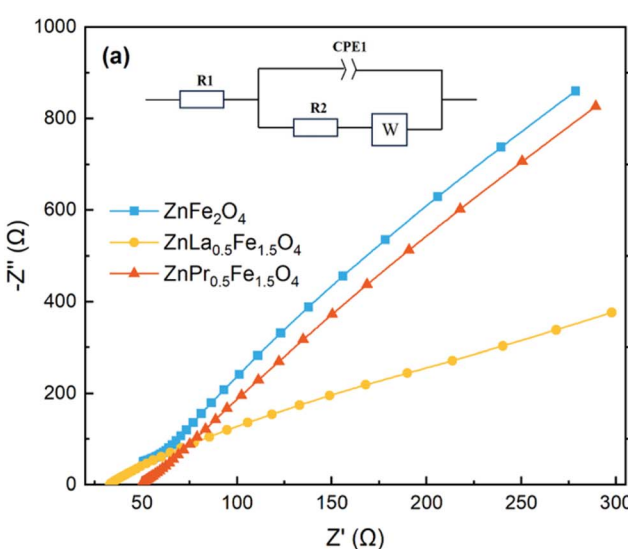


Fig. 7 EIS curves (a) and OCP curves (b) of different electrodes.



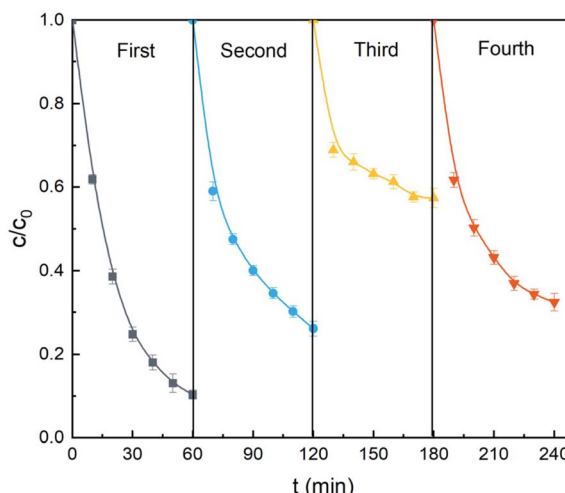


Fig. 8 The reusability of  $\text{ZnLa}_{0.5}\text{Fe}_{1.5}\text{O}_4$  for acetaminophen degradation. Reaction conditions:  $[\text{acetaminophen}]_0 = 20 \text{ mg L}^{-1}$ ,  $[\text{PMS}]_0 = 1.0 \text{ g L}^{-1}$ ,  $[\text{catalyst}]_0 = 1.0 \text{ g L}^{-1}$ , unadjusted pH = 6.98,  $T = 25^\circ\text{C}$ .

largest, which was contributed to the highest degradation efficiency of acetaminophen.

Overall, the oxidation of ROS and the direct electron transfer were responsible for the degradation of acetaminophen. More importantly, based on the above comparative studies, it could be concluded that La/Pr doping enhanced the content of oxygen vacancies in  $\text{ZnFe}_2\text{O}_4$ , and the enriched oxygen vacancies promoted the generation of ROS and accelerated the electron transfer in the system, and thus improved the degradation rate of acetaminophen.

### 3.4. Practical application potential assessment

In order to evaluate the potential of practical applications of  $\text{ZnLa}_{0.5}\text{Fe}_{1.5}\text{O}_4$ , its reusability, actual water environment adaptability and universality were investigated. Firstly, the reusability of  $\text{ZnLa}_{0.5}\text{Fe}_{1.5}\text{O}_4$  was evaluated in the four continuous cycling tests. No regeneration method was carried out in the first three cycles, and the used  $\text{ZnLa}_{0.5}\text{Fe}_{1.5}\text{O}_4$  was heat-treated 2 h at  $500^\circ\text{C}$  before the fourth cycle. As presented in Fig. 8, the degradation efficiency towards acetaminophen was 89.7%, 73.9% and 42.6% in the first, second and third cycle, respectively. The decrease of catalytic performance could be caused by the occupation of active sites by intermediate products and the unavoidable loss of catalyst in the recovery process.<sup>19,20</sup> The acetaminophen degradation efficiency was 67.5% in the fourth cycle, which indicated that the heat-treatment could lead to a partial recovery of the catalytic performance of  $\text{ZnLa}_{0.5}\text{Fe}_{1.5}\text{O}_4$ .

To examine whether  $\text{ZnLa}_{0.5}\text{Fe}_{1.5}\text{O}_4$  could be satisfactorily applied to actual water environment, the acetaminophen degradation in tap water and lake water (collected from the Mingde Lake in Tongren University, Tongren, China) was also conducted. As shown in Fig. 9, the removal efficiency of acetaminophen followed the order of lake water < tap water < ultrapure water. The decrease of the acetaminophen removal

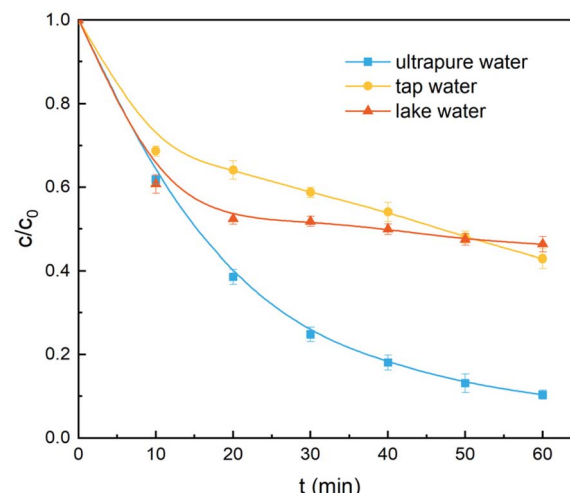


Fig. 9 The degradation of acetaminophen in different waterbodies. Reaction conditions:  $[\text{acetaminophen}]_0 = 20 \text{ mg L}^{-1}$ ,  $[\text{PMS}]_0 = 1.0 \text{ g L}^{-1}$ ,  $[\text{catalyst}]_0 = 1.0 \text{ g L}^{-1}$ , unadjusted pH = 6.98,  $T = 25^\circ\text{C}$ .

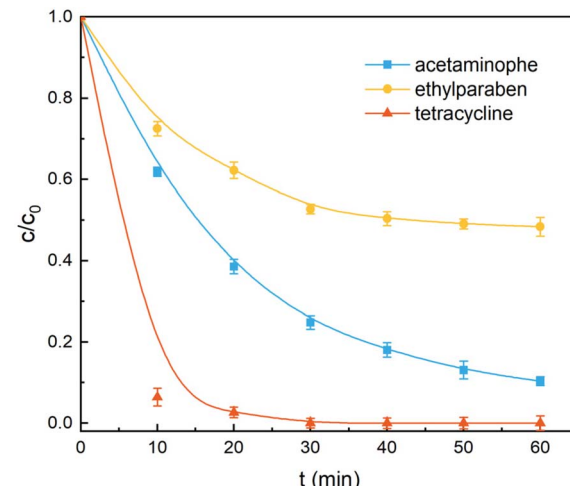


Fig. 10 Removal of various PPCPs using  $\text{ZnLa}_{0.5}\text{Fe}_{1.5}\text{O}_4/\text{PMS}$  system. Reaction conditions:  $[\text{acetaminophen}]_0 = [\text{ethylparaben}]_0 = [\text{tetracycline}]_0 = 20 \text{ mg L}^{-1}$ ,  $[\text{PMS}]_0 = 1.0 \text{ g L}^{-1}$ ,  $[\text{catalyst}]_0 = 1.0 \text{ g L}^{-1}$ , unadjusted pH,  $T = 25^\circ\text{C}$ .

efficiency could be due to the existence of  $\text{Cl}^-$  in the tap water and the existence of humic substances and  $\text{Cl}^-$  in and lake water.<sup>21,22</sup>

The universality of  $\text{ZnLa}_{0.5}\text{Fe}_{1.5}\text{O}_4$  catalyst was evaluated through the degradation of different PPCPs in  $\text{ZnLa}_{0.5}\text{Fe}_{1.5}\text{O}_4/\text{PMS}$  system. It could be seen from Fig. 10 that tetracycline could be completely degraded within 30 min. Although the removal rate of ethylparaben was 51.6%, it could be further improved under the optimal reaction conditions. These results indicated  $\text{ZnLa}_{0.5}\text{Fe}_{1.5}\text{O}_4/\text{PMS}$  system was effective and possessed potential application in the degradation of other PPCPs.

### 3.5. Determination of intermediates and toxicity estimation

The possible degradation pathway of acetaminophen in  $\text{ZnLa}_{0.5}\text{Fe}_{1.5}\text{O}_4/\text{PMS}$  system was proposed based on the liquid



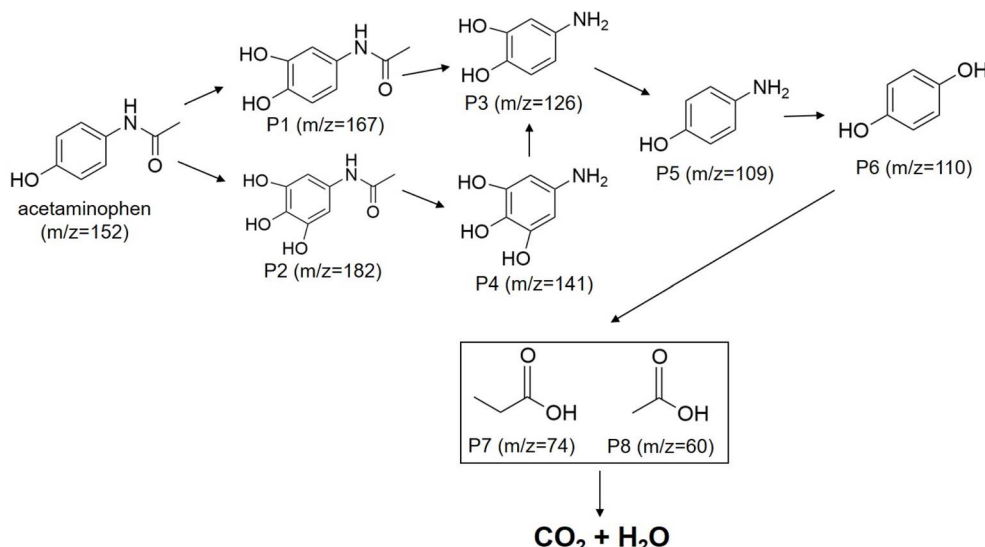


Fig. 11 Possible degradation pathways of acetaminophen in  $\text{ZnLa}_{0.5}\text{Fe}_{1.5}\text{O}_4/\text{PMS}$  system.

chromatography-mass spectrography (LC-MS) analysis. As shown in Fig. 11, the acetaminophen ( $m/z = 152$ ) was directly attacked by  $\cdot\text{OH}$ , resulting in the formation of P1 ( $m/z = 167$ ) and P2 ( $m/z = 182$ ).<sup>11</sup> Then,  $\text{O}_2^{\cdot-}$  attacked the C-N bond of P1 and P2, and the acetyl group was removed to form P3 ( $m/z = 126$ ) and P4 ( $m/z = 141$ ), respectively.<sup>12</sup> P3 and P4 were converted to P5 ( $m/z = 109$ ) under sustained ROS attack, and the amino group of P5 was oxidized to form P6 ( $m/z = 110$ ). Subsequently, P6 was ring-opened to produce P7 ( $m/z = 74$ ) and P8 ( $m/z = 60$ ). Finally, these small carboxylic acids were mineralized to form  $\text{CO}_2$  and  $\text{H}_2\text{O}$ .

The toxicities of acetaminophen and the eight intermediates were evaluated by Toxicity Estimation Software Tool (TEST). As presented in Fig. S4 in the SI, the original BHA exhibited “developmental toxicant”. After degradation in  $\text{ZnLa}_{0.5}\text{Fe}_{1.5}\text{O}_4/\text{PMS}$  system, the developmental toxicity values of P3, P4, P5, P6, P7 and P8 were smaller than that of acetaminophen. These results indicated that the overall toxicity of acetaminophen could be weakened by using  $\text{ZnLa}_{0.5}\text{Fe}_{1.5}\text{O}_4/\text{PMS}$  system.

## 4. Conclusion

In conclusion, rare earth ions were used to partly substitute  $\text{Fe}^{3+}$  in B-site, and La/Pr-doped  $\text{ZnFe}_2\text{O}_4$  was successfully prepared and used to activating PMS for the degradation of acetaminophen. The catalytic performance of  $\text{ZnFe}_2\text{O}_4$ ,  $\text{ZnLa}_{0.5}\text{Fe}_{1.5}\text{O}_4$  and  $\text{ZnPr}_{0.5}\text{Fe}_{1.5}\text{O}_4$  nanoparticles presented a positive correlation with the content of their oxygen vacancies.  $\text{ZnLa}_{0.5}\text{Fe}_{1.5}\text{O}_4$  with the highest amount of oxygen vacancies showed the highest catalytic activity, allowing an 89.7% removal efficiency of acetaminophen within 60 min. Both the characterizations and electrochemical analysis indicated the enhanced catalytic activity could be ascribed to the promotion of generated ROS and the acceleration of the electron transfer in the system. Moreover, the reusability experiments indicated that the degradation efficiency of acetaminophen decreased from 89.7%

to 42.6% in the third cycle, and the heat-treatment could lead to a partial recovery of the catalytic performance of  $\text{ZnLa}_{0.5}\text{Fe}_{1.5}\text{O}_4$ .

This work demonstrated that tuning the oxygen vacancies induced by La/Pr doping was a feasible strategy for enhancing the catalytic activity of  $\text{ZnFe}_2\text{O}_4$ , which provided a theoretical basis for the improvement of catalytic performance by doping of metals. The  $\text{ZnLa}_{0.5}\text{Fe}_{1.5}\text{O}_4/\text{PMS}$  system showed enormous potential for treating PPCPs in water. However, further studies, such as the optimum doping content and the performance of  $\text{ZnLa}_{0.5}\text{Fe}_{1.5}\text{O}_4$  in the treatment of real wastewater remain to be investigated.

## Conflicts of interest

The authors declare that they have no conflicts of interest.

## Data availability

The corresponding author will provide access to all the data used to support this research upon receiving an adequate request.

Supplementary information includes Text S1: the sourcing and purity information of the used chemicals in this study; Text S2: the detailed information including instruments and methods used in catalyst characterization; Text S3: the detailed experimental procedure for the recycle study; Text S4: the analytical methods; Text S5: the details of operational approach of electrochemical impedance spectroscopy (EIS) and open-circuit potential (OCP); Fig. S1: synthesis schematic depiction; Fig. S2: the adsorption of acetaminophen by different catalysts; Fig. S3: the XPS survey spectra; Fig. S4: toxicity estimation. See DOI: <https://doi.org/10.1039/d5ra05044h>.



## Acknowledgements

The authors would like to acknowledge the financial support from National Natural Science Foundation of China (22166031, 22266030), Department of Education of Guizhou Province (QJJ [2022]055 and QJJ[2022]003), Sichuan Science and Technology Program (2025YFHZ0312), Guizhou Provincial Science and Technology Projects (QKHC[G2023]ZD008) and Tongren city Science and Technology Projects (TSKY[2023]70).

## References

- 1 A. Hassani, J. Scaria, F. Ghanbari and P. V. Nidheesh, *Environ. Res.*, 2023, **217**, 114789.
- 2 K. Zhu, J. Wang, Y. Wang, C. Jin and A. S. Ganeshraja, *Catal. Sci. Technol.*, 2016, **6**, 2296–2304.
- 3 Y. Ren, L. Lin, J. Ma, J. Yang, J. Feng and Z. Fan, *Appl. Catal., B*, 2015, **165**, 572–578.
- 4 H. Lin, S. M. Li, B. Deng, W. Tan, R. Li, Y. Xu and H. Zhang, *Chem. Eng. J.*, 2019, **364**, 541–551.
- 5 H. D. Qin, H. Cheng, W. Shi, S. Z. Wu, J. Chen, J. M. Huang and H. Li, *J. Environ. Chem. Eng.*, 2023, **11**, 109070.
- 6 R. Yu, J. Zhao, Z. Zhao and F. Cui, *J. Hazard. Mater.*, 2020, **390**, 121998.
- 7 H. D. Qin, J. N. Hao, Y. Wang, J. M. Huang, J. Chang, G. Yang, B. Xing, S. Z. Wu and J. Chen, *RSC Adv.*, 2025, **15**, 11045.
- 8 H. D. Qin, J. N. Hao, H. Cheng, J. M. Huang, S. Z. Wu, J. Chen and W. Shi, *Chem. Eng. J.*, 2024, **494**, 152901.
- 9 K. Chu, F. Liu, J. Zhu, H. Fu, H. Zhu, Y. Zhu, Yu Zhang, F. Lai and T. Liu, *Adv. Energy Mater.*, 2021, **11**, 2003799.
- 10 P. Ni, S. Ma, N. Ma, C. Xu, G. Fan, J. Guo, J. Wei and J. Liu, *J. Alloy. Compd.*, 2024, **1002**, 175392.
- 11 X. Mu, D. Wang, D. He, J. Sun, X. Pan, Y. Zeng and H. Luo, *J. Environ. Chem. Eng.*, 2025, **13**, 115760.
- 12 T. Dang, G. Lu, M. Wang, Y. Ji, Y. Che and R. Jiang, *Process Saf. Environ.*, 2025, **199**, 107213.
- 13 Y. Huang, J. Zhang, Z. Guo, H. Zang, M. Zheng, T. Hao and J. Wei, *Environ. Res.*, 2025, **270**, 121013.
- 14 C. Du, C. Zhong, H. Xu, S. Zhang, H. Chen and Q. Xu, *Chem. Eng. Sci.*, 2025, **311**, 121604.
- 15 H. Zhang, C. Li, L. Lyu and C. Hu, *Appl. Catal., B*, 2020, **270**, 118874.
- 16 Y. Chen, X. Bai, Y. Ji and D. Chen, *J. Hazard. Mater.*, 2023, **441**, 129912.
- 17 P. Liang, D. Meng, Y. Liang, Z. Wang, C. Zhang, S. Wang and Z. Zhang, *Chem. Eng. J.*, 2021, **409**, 128196.
- 18 M. Li, Z. He, H. Zhong, W. Sun, L. Hu and M. Luo, *Chem. Eng. J.*, 2022, **441**, 136024.
- 19 Y. Lei, C. Chen, Y. Tu, Y. Huang and H. Zhang, *Environ. Sci. Technol.*, 2015, **49**, 6838–6845.
- 20 T. Zhang, H. Zhu and J. Croué, *Environ. Sci. Technol.*, 2013, **47**, 2784–2791.
- 21 Y. You, Z. K. Shi, Y. H. Li, Z. J. Zhao, B. He and X. W. Cheng, *Sep. Purif. Technol.*, 2021, **272**, 118889.
- 22 Y. Lia, S. Ma, S. Xu, H. Fu, Z. Li, K. Li, K. Sheng, J. Du, X. Lu, X. Li and S. Liu, *Chem. Eng. J.*, 2020, **387**, 124094.

